

The Bayesian Spatial Bradley–Terry Model: Urban Deprivation Modelling in Tanzania

Rowland G. Seymour, David Sirl, Simon P. Preston, Ian L. Dryden

School of Mathematical Sciences, University of Nottingham, UK

Madeleine J. A. Ellis, Bertrand Perrat, James Goulding

N/LAB, University of Nottingham, UK

Summary. Identifying the most deprived regions of any country or city is key if policy makers are to design successful interventions. However, locating areas with the greatest need is often surprisingly challenging in developing countries. Due to the logistical challenges of traditional household surveying, official statistics can be slow to be updated; estimates that exist can be coarse, a consequence of prohibitive costs and poor infrastructures; and mass urbanisation can render manually surveyed figures rapidly out-of-date. Comparative judgement models, such as the Bradley–Terry model, offer a promising solution. Leveraging local knowledge, elicited via comparisons of different areas’ affluence, such models can both simplify logistics and circumvent biases inherent to house-hold surveys. Yet widespread adoption remains limited, due to the large amount of data existing approaches still require. We address this via development of a novel Bayesian Spatial Bradley–Terry model, which substantially decreases the amount of data comparisons required for effective inference. This model integrates a network representation of the city or country, along with assumptions of spatial smoothness that allow deprivation in one area to be informed by neighbouring areas. We demonstrate the practical effectiveness of this method, through a novel comparative judgement data set collected in Dar es Salaam, Tanzania.

Keywords: Comparative Judgement, Preference Learning, Citizen Science, Networks

1. Introduction

Deprivation statistics are used by governmental and non-governmental organisations to describe the standard of living in a small administrative areas (McLennan et al., 2019). Yet assessment of deprivation depends not only on the financial situation of those living in an area, but also factors such as health, housing, commercial activity, and access to education. If correctly estimated, such statistics can be central to the design of successful policy interventions; supporting citizens and guiding decision makers in local government, non-governmental organisations and the business-sector alike. However, obtaining deprivation estimates is often a surprisingly challenging task, particularly in developing countries. In such contexts traditional household surveys are often prohibitively expensive or logistically intractable. Data collection efforts are impaired by poor physical infrastructures restricting sample sizes. Mass urbanization can render estimates rapidly out-of-date; and a lack of financial transparency in the face of vast informal economies exacerbates the well-established response biases inherent to household surveying (Randall and Coast, 2015; Lynn and Clarke, 2002).

In Africa, according to the World Bank’s chief economist, such issues have generated a “statistical tragedy” (Devarajan, 2013). Dar es Salaam, the largest city in Tanzania, is a case in point. With a population of over 6 million the city has doubled in size in just a decade, leaving official statistics generated but 5 years ago broadly inapplicable. The United Nations has estimated that the annual growth rate of the city will continue to be 4.8%, and by 2030 Dar es Salaam will be home to at least 10 million people (United Nations Department of Economic and Social Affairs, 2019). Experiencing such rapid growth means citizens lack resources, with poor physical infrastructures and absent public services resulting in a low quality of living. Over 70% of citizens in Dar es Salaam live in unplanned settlements and slums (Limbumba and Ngware, 2016), water sources in the city are polluted (Napacho and Manyele, 2010) and outbreaks of diseases are common (McCrickard et al., 2017). Determining the level of deprivation in each part of this rapidly changing city is key to designing policies and strategies to alleviate these issues, especially in the face of limited resources, yet traditional household surveys are simply not viable (Randall and Coast, 2015).

Citizen science and comparative judgement offer a way to address the lack of official data and rapid changes in the city, providing access to informed and up-to-date opinions from local citizens. Comparative judgement methods contrast sharply with traditional surveying approaches, in which a respondent might be asked to indicate the affluence level of an area, or their own household income, based upon some arbitrary scale. Instead, individuals are shown pairs of areas and asked which is the more affluent of the two. Making pairwise comparisons is preferable to making absolute judgements, which are well-evidenced as subject to strong biases and inconsistencies (Kalton and Schuman, 1982). With household income levels often being highly volatile in developing world contexts, and local populations often reticent to provide accurate response due to the scale of the informal economy (Randall and Coast, 2015), this also provides scope to reduce response bias and logistical costs.

To achieve this one might fit a Bradley–Terry (BT) model (Bradley and Terry, 1952) to pairwise comparative judgement data. This allows not only areas to be ranked, but deprivation levels in each neighbourhood or region to be estimated. However, existing models still require an obstructively large number of individual comparisons to be provided in order to produce accurate estimates. With data collection infrastructures remaining poor in developing countries (see, e.g., van Etten et al., 2019; Engelmann et al., 2018), comparative judgement solutions can only become viable in practice if the amount of data required can be reduced. We address this key issue via development of a novel Bayesian Spatial Bradley–Terry (BSBT) model, which substantially decreases the amount of data comparisons required for convergence. This model integrates a network representation of the city or country, along with assumptions of spatial smoothness that allow deprivation in one area to be informed by neighbouring areas.

Adding structure by including covariates in the standard BT model has only generally been achieved in a parametric framework with a linear predictor (see, e.g., Springall, 1973; Stern, 2011), although some nonparametric methods have tentatively been explored. A more flexible spline-based approach for explanatory variables has been proposed by de Soete and Winsberg (1993). A semi-parametric approach, which allows for subgroups within the set of objects being compared, has also been developed (Strobl

et al., 2011). However, these methods are unsuitable for spatial explanatory variables, as linear predictors cannot describe complex spatial structure. We instead avoid specifying any parametric functions and use a multivariate normal prior distribution to model the spatial structure. This novel treatment allows for far more flexibility as we do not need to propose strict parametric models, which often do not describe well the latent structure. We also extend the BSBT model to include ways to examine if different groups of judges hold different opinions. In developing countries, we are particularly interested in the differing opinions of men and women, as women can face starkly different health, social and economic difficulties to men. The BSBT model with judge information allows us to locate areas where men and women hold notably different opinions about the deprivation level.

1.1. Empirical Background

To demonstrate the practical effectiveness of this new method, we have additionally collected a large, novel comparative judgement data set to infer deprivation in Dar es Salaam. We include the data set in the BSBT R package that accompanies the paper, as well as in the supplementary material. The Dar es Salaam comparative judgement data set contains 75,078 comparisons made by 224 local participants, which we refer to henceforth as judges, as well as the gender of each judge. Dar es Salaam is divided into 452 administrative areas called *subwards*, which are the lowest level of administrative division in the city. To carry out the judgements, we designed a computer interface (see Figure 1) that showed judges images of pairs of subwards and allowed them to do one of: i) choose which of the subwards was more affluent, ii) indicate that they could not decide which was more affluent, or iii) indicate that they did not know one of the subwards.

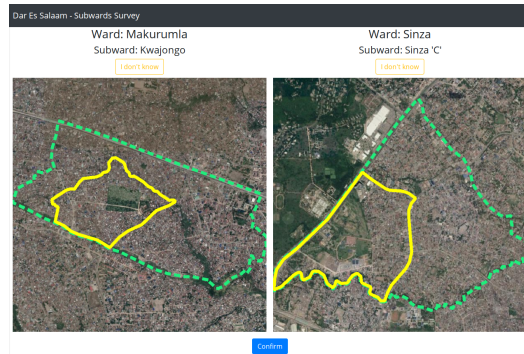


Fig. 1. A screenshot of the software designed to carry out the comparative judgement study. In this example a user is asked to choose the most affluent between two subwards, *Kwajongo* and *Sinza C*. Images were zoomable, with both the subward and ward named directly in order to contextualise the user.

Judges were recruited through word of mouth by students at local universities, NGOs and also via a local taxi driver association. The rationale for recruiting these judges was that they were all citizens of Dar es Salaam with a wide working knowledge of different subwards in the city. Data was collected *in situ* over two weeks in August 2018 via

17 data collection sessions each lasting two hours. Sessions were run in the morning, early and late afternoon, and evening to ensure as many judges as possible could attend. Judges were only allowed to attend one session. At the start of each session, the judges received a 15 minute training session in English and Swahili explaining how to make judgements and guidance on how to judge areas based on affluence and deprivation. Accompanying written instructions for the judges were provided in English and Swahili. A total of 14.6% of the comparisons made in the study were tied comparisons, meaning that the judge could not distinguish between the affluence levels in the two subwards. There are several ways of dealing with tied comparisons (see, e.g., Rao and Kupper, 1967; Turner and Firth, 2012); we randomly assigned one of the pair to be the more deprived subward.

An important aim of this work is to develop methodology that enables more efficient data collection, able to overcome the organisational challenges faced in the field. Two weeks were invested in collecting this large data set, and organisation and recruitment of participants prior to the study took several months. A key aim of the scale of the data collection process undertaken, was to conclusively evidence for future efforts that the first two days could have been sufficient if improved modelling procedures are employed - saving considerable time and resources in both collecting the data and reducing the number of participants needed to recruit, train and organise in the future.

2. A spatial framework for the Bradley–Terry model

2.1. The standard Bradley–Terry model

Consider a comparative judgement data set consisting of K pairwise comparisons of N areas. We assign to each area what we call a *relative deprivation parameter* $\lambda_i \in \mathbb{R}$ ($i = 1, \dots, N$) and infer the value of each parameter using a comparative judgement model. A large positive value of λ_i indicates a very affluent area and a large negative value indicates a very deprived area.

We begin by outlining the standard BT model, a commonly used comparative judgement model. If areas i and j are compared n_{ij} times, the number of times area i is judged to be more affluent than area j is modelled as

$$Y_{ij} \sim \text{Bin}(n_{ij}, \pi_{ij}),$$

and we assume Y_{ij} are independent. Here the probability π_{ij} that area i is judged to be more affluent than area j depends on the difference in relative deprivation of i and j and is

$$\text{logit}(\pi_{ij}) = \lambda_i - \lambda_j \iff \pi_{ij} = \frac{\exp(\lambda_i)}{\exp(\lambda_i) + \exp(\lambda_j)} \quad (i \neq j, 1 \leq i, j \leq N). \quad (1)$$

Model (1) is invariant to translations $\lambda_i \rightarrow \lambda_i + c$ (for any $c \in \mathbb{R}$), so an identifiability constraint is needed. A common choice is $\sum_{i=1}^N \lambda_i = 0$, which means that relatively deprived areas will have negative parameters, relatively affluent areas will have positive parameters and areas with middling levels of relative deprivation will have parameters near zero.

We write y_{ij} for the number of times area i was judged to be more affluent than area j , and denote by \mathbf{y} the set containing these outcomes for all pairs of areas. The likelihood function for the model is given by

$$\pi(\mathbf{y} \mid \lambda_1, \dots, \lambda_N) = \prod_{i=1}^N \prod_{j < i} \binom{n_{ij}}{y_{ij}} \pi_{ij}^{y_{ij}} (1 - \pi_{ij})^{n_{ij} - y_{ij}}. \quad (2)$$

We will compare our model to the standard BT model and the implementation provided in the **BradleyTerry2** R package (Turner and Firth, 2012), as this is a popular implementation of the method (see, e.g., Cattelan, 2012; Varin et al., 2016; Grinfeld et al., 2018). This package computes MLEs for the model parameters. Due to the identifiability constraint in the **BradleyTerry2** package, we cannot compute standard errors for all the estimates, and so we follow Turner and Firth (2012) and construct 95% confidence intervals using the quasi-variance for the estimates in the standard BT model, which is done using the **qvcalc** package (Firth, 2020).

2.2. The Bayesian Spatial Bradley–Terry model

In the BSBT model, we assume the relative deprivation parameters λ_i to be random and dependent on one another, with a higher level of dependence between nearby areas than areas which are further apart. To avoid making specific parametric assumptions about the level of deprivation in each area, we model the relative deprivation parameters using a multivariate normal prior distribution. We use a zero-mean multivariate normal prior distribution for the deprivation level parameters $\boldsymbol{\lambda} = \{\lambda_1, \dots, \lambda_N\}$ subject to the constraint $\mathbf{1}^T \boldsymbol{\lambda} = 0$, where $\mathbf{1} = (1, \dots, 1)^T$ is a vector of ones. This matches the condition in the standard BT model, that the sum of the deprivation levels is 0. Conditional on this constraint

$$(\boldsymbol{\lambda} \mid \mathbf{1}^T \boldsymbol{\lambda} = 0) \sim \text{MVN}(\mathbf{0}, \Sigma - \Sigma \mathbf{1}(\mathbf{1}^T \Sigma \mathbf{1})^{-1} \mathbf{1}^T \Sigma). \quad (3)$$

2.2.1. Modelling spatial covariance

The structure of the covariance matrix Σ is a modelling choice and there are number of options to choose from. In the simplest terms, we want to assign high covariance between deprivation levels in nearby subwards and low covariance between levels in distant subwards. A widely used option in Euclidean spatial domains is to use the squared-exponential covariance function (Rasmussen and Williams, 2006). Using this function, the covariance between the deprivation levels in subwards i and j is

$$\text{cov}(\lambda_i, \lambda_j) = \Sigma_{i,j} = k(i, j; \alpha, l) = \alpha^2 \exp\left(-\frac{d_{ij}^2}{l^2}\right), \quad (4)$$

where d_{ij} is the Euclidean distance between areas i and j , α^2 is the prior variance hyperparameter and l is the characteristic length scale, which describes what is meant by nearby and distant. However, using a function which is stationary in Euclidean space may not capture the change in deprivation in all parts of the city. The centre of cities are

typically densely packed with small areas, and peri-urban and rural areas being larger. Modelling the spatial structure using a Euclidean metric is therefore unsuitable since, for example, two points 1km apart in a rural area are likely similar, but two points 1km apart in a city centre may be very different.

Urban regions are typically divided into sub-areas for administrative purposes, and these neighbourhoods often provide natural units over which to quantify deprivation. While spatially connected, such areas often vary greatly in size. In this paper, we model an urban region as a network, whereby these low-level areas are represented as nodes with edges joining neighbouring areas, such that we can use a network-based (i.e. non-Euclidean) distance to define spatial ‘closeness’ between pairs of areas when defining prior assumptions of spatial smoothness. Using a network metric allows us to model nonstationary structures. We therefore begin by transforming the set of areas into a network by treating each area as a node and placing edges between adjacent areas; some modelling choices are required when dealing with noncontiguous areas or islands. In the Dar es Salaam network, we add two additional edges over the Kurasini creek to reflect the high-volume road and ferry connections. Figure 2 shows a map of Dar es Salaam and the corresponding network.

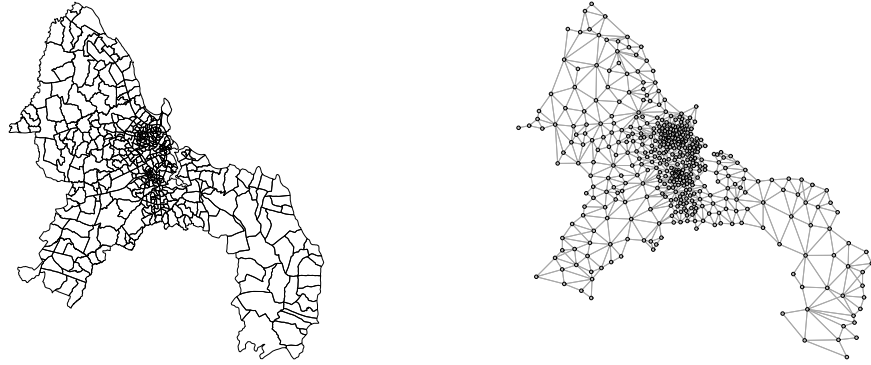


Fig. 2. A map and the network representation of subwards in Dar es Salaam.

We can adapt the squared exponential covariance function in (4) for use with a network by letting d_{ij} be the distance of the shortest path between subwards i and j . The shortest distance can be computed using Dijkstra’s algorithm (see, e.g., Cormen et al., 2001). Although using a network reduces the issue of stationarity, specifying the value of the length scale still may be challenging or restrictive; instead, when using the rational quadratic covariance function, which is a mixture of squared exponential covariance functions with different length scale values, we can specify the relative importance of long and short scale variation in deprivation. Another option is to use the Matérn covariance function, which would remove the assumption that the spatial structure is

smooth. However, using when the shortest-path network, the resulting matrix is not guaranteed to be positive semi-definite and we may need to project the matrix into the space of covariance matrices. This can be done in a number of ways, including setting the negative eigenvalues to 0 or modifying the polar decomposition (Higham, 1988).

Instead of using a distance based approach, we can construct the covariance matrix directly from the structure of the network. Estrada and Higham (2010) describe several options for quantifying the ‘communicability’ between two nodes of a network in terms of functions of the adjacency matrix of the network. The option we choose is based on the matrix exponential of the adjacency matrix as this measure emphasises connectedness over short distances rather than long distances to a greater extent than the alternatives described in Estrada and Higham (2010). Let $\Lambda = e^A$, where A is the network’s adjacency matrix, and let D be a diagonal matrix containing the elements on the diagonal of Λ . The covariance matrix is given by

$$\Sigma = \alpha^2 D^{-\frac{1}{2}} \Lambda D^{-\frac{1}{2}}, \quad (5)$$

where α^2 is a hyperparameter describing the variance in the deprivation levels. The matrix Σ therefore has diagonal entries α^2 and off-diagonal entries proportional to the communicability of each pair of subwards in the network. We thus achieve our aim of assigning higher covariance between better-connected pairs of subwards, using a natural characterisation of the network. Although we use the matrix exponential covariance matrix in the paper, we find no discernible difference in the results of Sections 3 and 4 when using the (network-adapted) squared-exponential covariance function.

2.3. Incorporating judge information

We now incorporate judge covariates into the model as this avoids the assumption that the judges act homogeneously. Suppose there are G groups of judges and let \mathbf{x}_g be the vector of length P containing the covariates for group g . We assume judges in the same group act homogeneously. The vector \mathbf{x}_g may contain categorical, discrete or continuous covariates or a mixture of all three; for a categorical covariate we represent the q levels of the covariate by q indicator functions. If \mathbf{x}_g contains categorical covariates the number of groups may be small, but if \mathbf{x}_g contains a continuous covariate each judge may be its own group.

We model the deprivation in area i , as perceived by judges in group g , to be

$$\lambda_i^g = \lambda_i + \sum_{p=1}^P x_p^g \beta_{pi},$$

where x_p^g is the p^{th} element of \mathbf{x}_g and β_{pi} is the parameter corresponding to x_p^g and area i , where $i = 1, \dots, N$. Modifying the likelihood function in equation (2) to take account of the contributions from each group of judges, we now have the likelihood function

$$\pi(\mathbf{y} \mid \boldsymbol{\lambda}, \boldsymbol{\beta}_1, \dots, \boldsymbol{\beta}_P) = \prod_{g=1}^G \prod_{i=1}^N \prod_{j < i} \binom{n_{ijg}}{y_{ijg}} \pi_{ijg}^{y_{ijg}} (1 - \pi_{ijg})^{n_{ijg} - y_{ijg}}, \quad (6)$$

where n_{ijg} is the number of times judges in group g compared areas i and j , y_{ijg} is the number of times judges in group g judged area i to be more affluent than area j , π_{ijg} is the probability judges in group g judge area i to be more affluent than area j and is given by $\text{logit}(\pi_{ijg}) = \lambda_i^g - \lambda_j^g$, and $\beta_p = \{\beta_{p1}, \dots, \beta_{pN}\}$ is the set of parameters corresponding to p^{th} element of the set of judge covariates. We recover the model and likelihood of Section 2.2 by taking $G = 1$ and $P = 0$ in this formulation.

As in the BSBT model with no judge covariates, we place a constrained multivariate normal prior distribution on the spatial parameters λ , shown in (3). We also place an independent, constrained, multivariate normal prior distribution on each β_p which allows us to model the effect of each covariate spatially. So that the deprivation parameters, λ , represent the grand mean of the deprivation for all judges, we enforce a second constraint amongst the set of parameters β_p , which correspond to a given categorical covariate, as this allows us to treat each category symmetrically, i.e. we avoid fixing one category as a reference category and then not having any uncertainty associated with it. For a group of q covariates representing the q categories of covariate p , the corresponding parameters $\beta_{p_1i}, \dots, \beta_{p_qi}$ need a constraint to ensure identifiability. We use $\beta_{p_1i} + \dots + \beta_{p_qi} = 0$ for each area $i = 1, \dots, N$.

An example of including judge information is investigating how judges of different genders view different subwards. In less developed countries, women may be more vulnerable to various forms of exploitation (e.g. female genital mutilation, modern slavery, and forced marriage) and finding areas women view as more deprived than men may indirectly give information about where these practices are happening. We sort the judges into two groups (i.e. $G = 2$), men and women. We let $\mathbf{x}_1^T = (1 \ 0)$ for male judges and $\mathbf{x}_2^T = (0 \ 1)$ for female judges (i.e. $P = 2$). The appropriate constraint to ensure identifiability is then $\beta_{1i} + \beta_{2i} = 0$ for each area i .

2.4. Fitting the model

Now we have described the BSBT model, we develop a Markov chain Monte Carlo (MCMC) algorithm to infer the model parameters given the observed comparative judgements \mathbf{y} , and the judge covariates \mathbf{x} . The model parameters are: the deprivation parameters λ , any covariate parameters β_p , and the covariance function variance hyperparameters α_λ^2 and $\alpha_1^2, \dots, \alpha_P^2$. By Bayes' theorem, the posterior distribution is

$$\begin{aligned} \pi(\lambda, \beta_1, \dots, \beta_P, \alpha_\lambda^2, \alpha_1^2, \dots, \alpha_P^2 \mid \mathbf{x}, \mathbf{y}) &\propto \pi(\mathbf{y} \mid \lambda, \beta_1, \dots, \beta_P) \pi(\lambda \mid \alpha_\lambda^2, \mathbf{1}^T \lambda = 0) \pi(\alpha_\lambda^2) \\ &\times \prod_{p=1}^P \pi(\beta_p \mid \alpha_p^2, \mathbf{1}^T \beta_p = 0) \pi(\alpha_p^2). \end{aligned} \quad (7)$$

The first term on the right hand side is the likelihood function (6) and the second term is the prior density for the spatial component λ , for which we use the constrained prior distribution (3). We place an independent prior distribution on the variance hyperparameter α_λ^2 , which is the third term on the right hand side. The product term contains the prior distributions for the covariate parameters β_1, \dots, β_P and the variance hyperparameters $\alpha_1^2, \dots, \alpha_P^2$ for these distributions.

The posterior density cannot be computed explicitly, but it can be sampled from using Algorithm 1. This MCMC algorithm involves iterating Gibbs updates for the variance hyperparameters, $\alpha_\lambda^2, \alpha_1^2, \dots, \alpha_P^2$, and Metropolis-Hastings updates for the spatial components, $\boldsymbol{\lambda}$ and β_1, \dots, β_P . For analytical convenience, we place a conjugate inverse-Gamma prior distribution on α_i^2 , the density function of which is

$$\pi(x; \chi, \omega) = \frac{\omega^\chi}{\Gamma(\chi)} \frac{1}{x^{\chi+1}} \exp\left(-\frac{\omega}{x}\right) \quad (x > 0; \chi > 0, \omega > 0).$$

The Gibbs updates are possible because the full conditional distribution for α_λ^2 has a closed form. It is given by

$$\alpha_\lambda^2 \mid \boldsymbol{\lambda} \sim \text{inv-}\Gamma\left(\chi + \frac{N}{2}, \omega + \frac{1}{2} \boldsymbol{\lambda} \bar{\Sigma}^{-1} \boldsymbol{\lambda}^T\right),$$

where $\bar{\Sigma}$ is the covariance matrix of the constrained prior with $\alpha^2 = 1$ in (5). Analogously, the full conditional distribution for α_p^2 is

$$\alpha_p^2 \mid \beta_p \sim \text{inv-}\Gamma\left(\chi + \frac{N}{2}, \omega + \frac{1}{2} \beta_p \bar{\Sigma}^{-1} \beta_p^T\right),$$

To update the deprivation parameters, $\boldsymbol{\lambda}$, we use a Metropolis-Hastings sampler with an underrelaxed proposal mechanism (Neal, 1998). This allows us to update the parameters as a block and reduces the computational complexity compared to updating each deprivation parameter individually. Given the current deprivation parameters $\boldsymbol{\lambda}$, we propose new values by

$$\boldsymbol{\lambda}' = \sqrt{1 - \delta^2} \boldsymbol{\lambda} + \delta \boldsymbol{\nu},$$

where $\delta \in (0, 1]$ is a tuning parameter and $\boldsymbol{\nu}$ is a draw from the constrained prior distribution in equation (3). We accept this proposal with probability

$$p_{\text{acc}} = \min\left(\frac{\pi(\mathbf{y} \mid \boldsymbol{\lambda}', \beta_1, \dots, \beta_P)}{\pi(\mathbf{y} \mid \boldsymbol{\lambda}, \beta_1, \dots, \beta_P)}, 1\right).$$

The proposal ratio using the underrelaxed proposal mechanism is the inverse of the prior ratio, meaning the acceptance probability is the ratio of the likelihood function with the proposed and current deprivation parameters. We follow an analogous process for the covariate parameters β_1, \dots, β_P .

2.5. Implementing the Model

We have developed an R package to allow any user to implement this method on a comparative judgement data set. The package BSBT is available on CRAN (Seymour and Briant, 2021). It includes the novel comparative judgement data set on deprivation in Dar es Salaam, Tanzania, shapefiles for the 452 subwards in the city and a vignette containing instructions on how to reproduce the analysis in section 4. The package allows users to place a constrained multivariate normal prior distribution for deprivation parameters over a predetermined network (it also facilitates constructing the network)

Algorithm 1 MCMC Algorithm for the BSBT Model

-
- 1: Choose initial values for λ , β_1, \dots, β_P and $\alpha_\lambda^2, \alpha_1^2, \dots, \alpha_P^2$.
On iteration j of the MCMC algorithm do
 - 2: Update λ_i using a Metropolis-Hastings step with underrelaxed proposal mechanism;
 - 3: Update β_1, \dots, β_P using a Metropolis-Hastings step with underrelaxed proposal mechanism;
 - 4: Update α_λ^2 using a Gibbs step;
 - 5: **for** i in 1 to P **do**
 - 6: Update α_i^2 using a Gibbs step;
 - 7: **end for**
-

and fit the model using an MCMC algorithm. We provide a number of covariance functions, including the squared-exponential, Matérn and matrix exponential functions. The MCMC functions included in the package can be used to fit either the spatial models, or spatial model with a covariate for judge gender. Due to our formulation of the likelihood function, the computational time for the BSBT implementation scales according to the number of areas, whereas the implementation provided in the **BradleyTerry2** package scales according to the number of comparisons.

3. Simulation Studies

We first investigate the effectiveness of our approach, both in accurately estimating deprivation levels and in reducing the amount of data required, through two simulation studies. The first is based on a synthetic one-dimensional ‘city’, which allows us to visualise the results. The second is based on a data set on deprivation levels in local authority areas in England.

3.1. A 1-d Study

We construct a one dimensional city, where the areas which are compared are points on the line. Although this is a simple toy example, it allows us to visualise the city and level of deprivation in each area. We draw the locations for 100 areas from a Laplace distribution with mean 0 and variance 8, as this gives a region near 0 which is densely packed with relatively small areas, and fewer but larger areas in the outlying parts of the city. We specify the level of deprivation in each area by the piecewise function

$$g(x) = \begin{cases} \sin(x) + x + \pi & \text{if } x < \pi, \\ \sin(4x) & \text{if } \pi \leq x \leq \pi, \\ \sin(x) - x + \pi & \text{if } x > \pi. \end{cases}$$

This gives a level of deprivation which changes quickly in the city centre compared to the outskirts.

We simulate the comparisons according to the model in equation (2) and choose pairs of areas uniformly at random to compare. We simulate data sets of various sizes to mimic real data collection. The sizes of simulated data sets used in this paper are

Table 1. Data set sizes used in the simulations studies, using 180 comparison per judge hour (the four largest sizes for 2-d study only).

Judge hours	1	2	5	10	25	50	100	250	500	1,000
Comparisons	180	360	900	1,800	4,500	9,000	18,000	45,000	90,000	180,000

shown in Table 3.1. We use ‘judge hours’ to quantify the number of comparisons by the total judging time required, assuming 20 seconds per comparison or 180 comparisons per judge hour. (In this 1-d study with fewer areas than the 2-d study in the next section, both models reach data saturation after 9,000 comparisons, so we do not use the four largest data sets.) To simulate comparisons we draw pairs of areas uniformly at random from all possible pairs.

We fit the BSBT model and run the MCMC algorithm for 500,000 iterations, removing the first 100,000 as a burn-in period. We estimate the quality of each area and learn plausible values of the variance hyperparameter α_λ^2 . We fix the tuning parameter $\delta = 0.01$, based on initial runs of the algorithm. For the prior distribution on α_λ^2 , we fix $\chi = \omega = 0.1$ which results in a somewhat noninformative distribution (Gelman, 2006). The top row of Figure 3 gives results for the BSBT model using 900 and 9,000 comparisons; it shows the true deprivation levels, the location of the areas and the posterior median deprivation with a 95% credible interval for each area. We see two main effects from increasing the number of comparisons. The first is increasing accuracy of inference, with better estimates and less uncertainty when using 9,000 comparisons. The second is the model’s ability to deal with extreme levels of deprivation, either very deprived or very affluent areas. The areas on the outskirts of the synthetic city make this a challenging data set for the BSBT model, since they are extreme both spatially and in terms of deprivation. When using smaller data sets, inferred deprivation levels in the BSBT model are pulled towards 0 by the prior distribution. As we do not have sufficient data to estimate the extent of the deprivation in the most extreme areas, we also underestimate the variance parameter. Although we do not accurately estimate the extent of the extremes, we do successfully identify which areas have extremes of deprivation.

Corresponding results from fitting the standard BT model to the same data sets are given in the bottom row of Figure 3. These plots show the same detail of the true deprivation and locations of areas, but here show MLEs and corresponding intervals based on quasi-variances. In the smallest data set there are some areas which feature in very few comparisons, so estimates for their level of deprivation are highly uncertain. This shows in the lower-left plot as intervals spanning all shown deprivation values and/or the point estimate not being visible on the scale used. Many estimates are also quite poor compared to the BSBT results. Here we see one of the main advantages of the BSBT model: including weak prior assumptions about spatial correlations allows it to learn about areas featured in very few, or even no, comparisons from information about nearby areas. Figure 3 also shows that when using the 9,000 comparisons the standard and BSBT models perform fairly similarly. This is expected since the data set is large enough to estimate the model parameters well using either model.

To assess the model fit, we compute the Mean Absolute Error (MAE) for the result

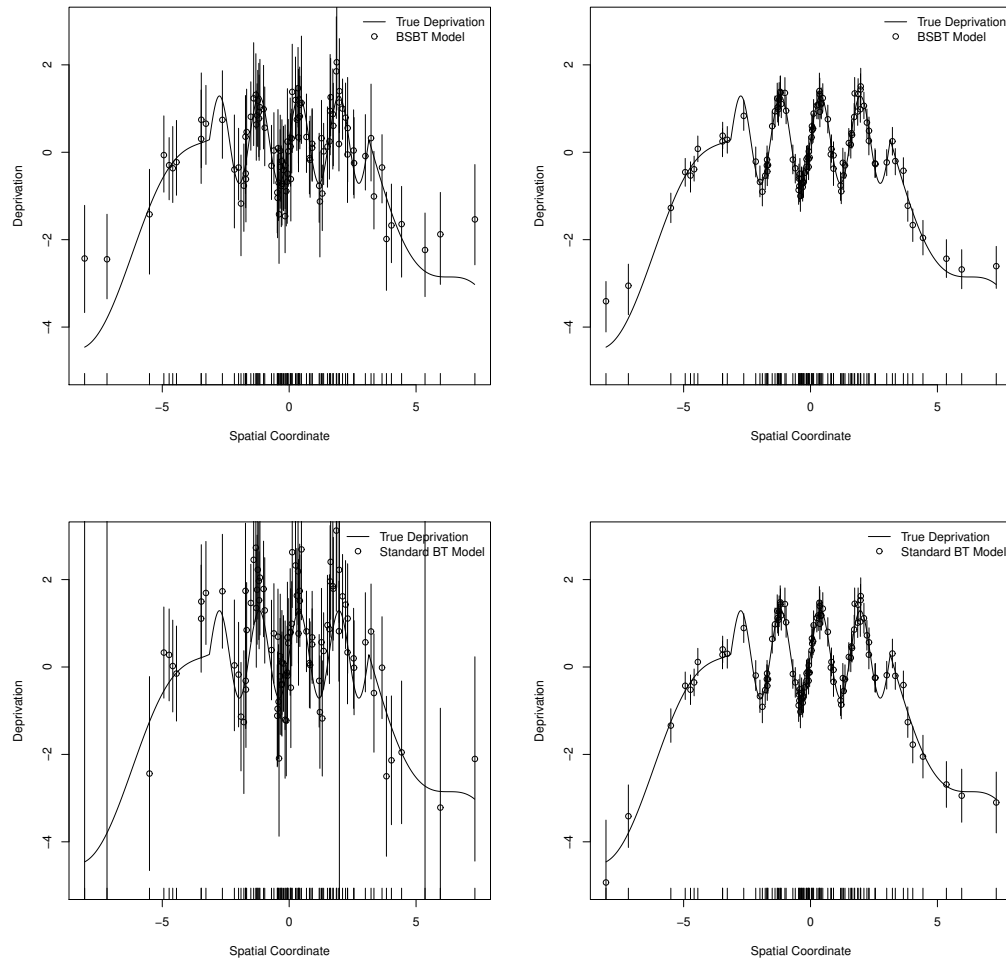


Fig. 3. Results for the 1-d simulation study using the BSBT and standard BT models. The top row shows the results of the BSBT model and the bottom row shows the results of the standard BT model. The left column shows the models fitted with 900 comparisons and the right column with 9,000 comparisons. The same scales are used on all plots for ease of comparison, but this means that in the bottom row some intervals are larger than can be displayed.

of each set of comparisons, which is given by

$$\text{MAE} = \frac{1}{N} \sum_{i=1}^N |\lambda_i - \hat{\lambda}_i|,$$

where $\hat{\lambda}_i$ is the estimate corresponding to the MLE or posterior median for area i . The left plot in Figure 4 shows the log MAE for each data set. The BSBT model performs better than the standard BT model in all cases (except for the two largest data sets, where the comparison space is saturated and, as discussed above, the models perform very similarly). Figure 4 also shows that when we fix the number of comparisons, the error in the BSBT model is always lower bound to error in the standard model, and predominantly reflects a large improvement. For example, when using 900 comparisons, MAE in the BSBT model (0.418) is less than half that in the standard model (0.975). The level of error in the standard model with 1,800 comparisons is of the same order as the BSBT model with 900 comparisons, demonstrating that with the BSBT model we can collect appreciably less data without compromising the quality of the estimates. In small data sets we cannot compute the MLE for areas which are not featured in any comparisons. As such, when using 180 comparisons we are unable to compute the MAE for the standard BT model. The BSBT model does not suffer from this issue since it uses a correlated prior distribution, so we still get an estimate of deprivation for these areas, albeit with large uncertainty.

3.2. A 2-d study

To assess the model’s ability to infer data generating deprivation levels in more realistic scenarios, we simulate deprivation levels for the subwards in Dar es Salaam by drawing a sample from the prior distribution, then seek to infer these from simulated comparative judgements. A map of the city and the corresponding network are shown in Figure 2. We simulate data sets of the sizes given in Table 3.1. We fit the model to each data set, running the MCMC algorithm for 1,500,000 iterations and removing the first 500,000 iterations as a burn-in period.

The right plot of Figure 4 shows the log MAE for each data set. The BSBT model again outperforms the standard model for all sizes of data set used. For a fixed number of comparisons, the BSBT model has smaller error than the standard model. For example, when using 1,800 comparisons (10 judge hours), MAE using the BSBT model (0.260) is less than a third of the error in the standard model (0.907). This figure also shows that, by using the BSBT instead of the standard BT model, we can substantially reduce the number of comparisons required to achieve a given level of error. For example, MAE in the BSBT with 5 judge hours is similar to that in the standard model with 50 judge hours, a decrease in judge hours of 90%; and 250 judge hours with the standard model yields similar MAE to 100 judge hours with BSBT, a still substantial reduction of 60% in terms of the data required to give a similar level of performance. This much greater reduction than observed in the 1-d study derives in part from the dimension of the spatial domain being considered: areas will tend to have more neighbours in 2-d than in 1-d, so the benefit of modelling spatial correlations is enhanced. As in the 1-d study, for small

data sets we are unable to compute the MLE for all areas and so the corresponding MAE is undefined for the standard BT model.

We observe in both this simulation study and the 1-d simulation study that the performance of the BT and BSBT models are very similar when the number of judgments is large. This is to be expected from the Bernstein-von Mises theorem (Kleijn and van der Vaart, 2012) whereby the posterior distribution of finite dimensional parameters and the MLEs tend to the same asymptotic multivariate normal distribution for large samples, subject to smoothness and identifiability conditions on the prior distribution and a positivity condition on the prior at the true value.

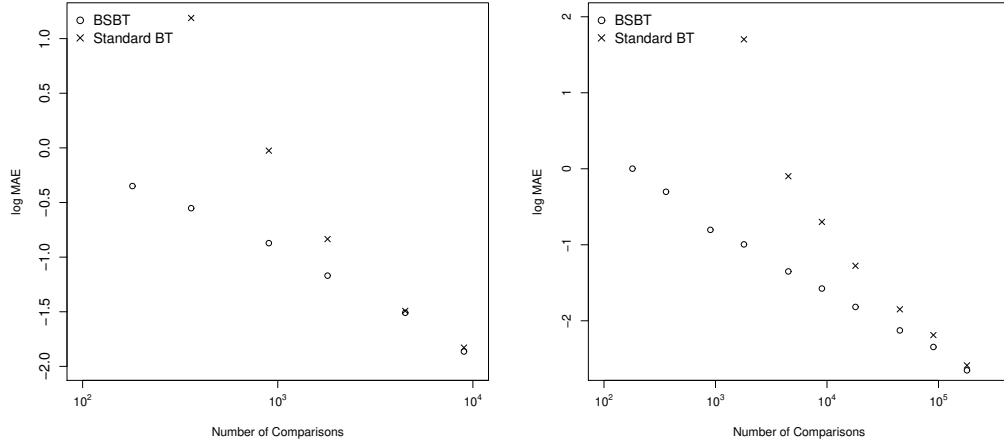


Fig. 4. Log MAE for the simulation studies, comparing performance of the standard BT and the BSBT models in terms of error as a function of the number of comparisons. Left: 1-d study of Section 3.1. Right: Synthetic Dar es Salaam study of Section 3.2.

4. Deprivation in Dar es Salaam, Tanzania

4.1. Bayesian Spatial Bradley–Terry Model

We fit the BSBT model to the data and run the MCMC algorithm shown in algorithm 1 for 1,500,000 iterations, removing the first 500,000 iteration as a burn-in period. This took around 3 hours on a standard desktop PC. We examined trace plots to ensure adequate mixing of the Markov chain and to choose the length of the burn-in period. These are given in the supplementary material. We fix the tuning parameter $\delta = 0.01$, based on initial runs of the algorithm, and the inverse gamma prior distribution parameters $\chi = \omega = 0.1$. The estimates for the level of deprivation in each subward in the city are shown in Figure 5. We see a north-south trend, whereby the level of deprivation increases further south in the city. We find several sharp changes in deprivation in the city centre, where slums neighbour affluent subwards. The most affluent subward is Masaki, and the ten most affluent areas are all concentrated around the Masaki peninsula directly

north of the city centre and home to most of the affluent expatriate communities. The ten most deprived subwards are geographically spread out, with one, Mpakani, being located in the centre of Dar es Salaam and the others spread across the outer regions of the city. Four of the ten most deprived subwards are in the Somangila ward, a coastal ward in the east of the city.

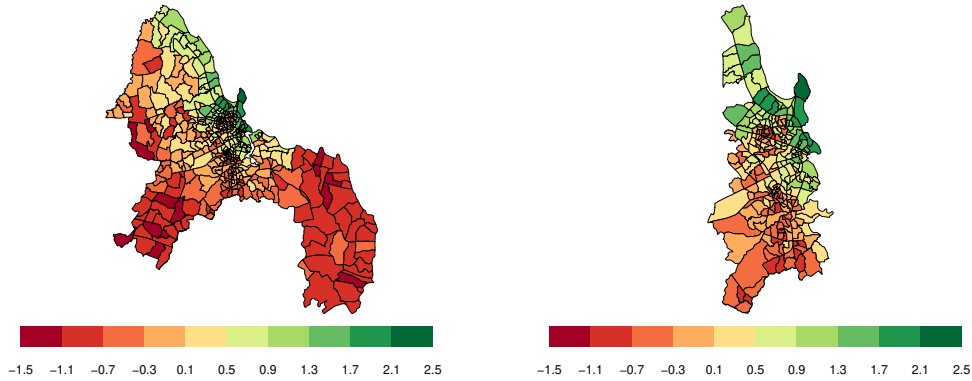


Fig. 5. The posterior mean values for the BSBT model applied to the Dar es Salaam data set. The figure on the right shows a magnified section of the centre of the city.

The uncertainty in the estimates for the level of deprivation in each subward differs considerably, as shown in Figure 6. We see a correlation between the level of uncertainty in our estimate and the estimated level of deprivation. As the most affluent areas tend to also be well known areas, such as tourist resorts or areas with government buildings, we were able to collect more comparisons involving these subwards and therefore there is less uncertainty in our estimates for the deprivation in these areas. We also estimate the variance parameter α_λ^2 ; its posterior mean is 3.378 with 95% credible interval (2.868, 3.993) and the posterior distribution is shown in Figure 6. See also Section 2 of the Supplementary Material, which gives some diagnostic information for the MCMC.

For the full data set, results for the standard BT and BSBT models are very similar due to the large amount of data in this data set (see Section 1 of the Supplementary Material). We see little difference in both the inferred deprivation levels and the uncertainty around the estimates. However, the data set that we have is quite large, so this is likely a data saturation effect (cf. Figure 4); an important aim of our work is to investigate if much fewer comparative judgements could have been collected, at a much reduced cost, with little loss of information.

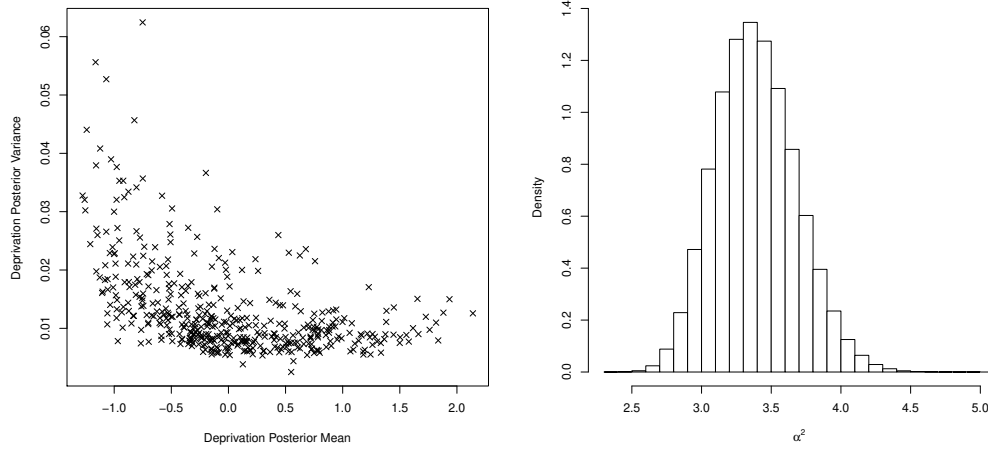


Fig. 6. Uncertainty in the fitted BSBT model for the Dar es Salaam data set. Left: The estimated level of deprivation in each subward against the uncertainty in the estimate. Right: The posterior distribution for the variance parameter α_λ^2 .

4.2. Efficiency of the BSBT model

To investigate the effectiveness of the model when we have a smaller number of comparisons, we also fit both the standard BT and BSBT models to the comparisons collected on the first two days of the field work. This subset includes 13,361 comparisons (around 18% of the original data set) and we compute the MAE taking the true values to be the inferred deprivation levels using the full data set. Using the BSBT model on this roughly halves the MAE compared to the standard BT model, reducing it from 0.523 to 0.267. Alongside the analysis shown in Figure 4, this shows that by using the BSBT model, in future we can collect far fewer comparisons yet attain similar levels of error in the results. This will reduce the time and cost associated with data collection in similar future fieldwork.

4.3. Gender Differences in Dar es Salaam

For the Dar es Salaam data, there were 91 female judges and 133 male judges. For reasons outlined in the introduction we are interested in determining whether different genders have different perceptions of some parts of the city. Our first observation is each male judge did on average 328 comparisons, whereas the average among female judges was 200. This is because the women took longer to carry out individual comparisons than the men. Another difference is that the women tended to be familiar with fewer subwards than the men, perhaps suggesting they are less mobile in the city. We fit the BSBT model with gender effect to the data, here $G = 2$ as we sort comparisons into two groups (men and women) and $P = 2$ as we model the effect of being male or female. We run the MCMC algorithm for 5,000,000 iterations, which took one day on a standard desktop PC. Diagnostic plots can be found in Section 3 of the Supplementary Material.

We fix $\delta = 0.01$ based on initial runs of the algorithm. We estimate the variance α_λ^2 (for λ) to be 3.846 (95% CI: (3.073, 3.694)) and α_1^2 (for β_1) 0.026 (95% CI: (0.002, 0.034)). Such a small value of α_1^2 suggests the men's and women's perceptions are highly correlated.

Figure 7 shows the distribution of the posterior mean deprivation levels perceived by men and women. We see that the distribution of the levels of deprivation perceived by men and women are largely the same. We also show posterior density estimates for men and women's perceptions of two subwards. In Kibonde Maji A, a somewhat deprived subward in the south of the city on a trunk road, there is no perceptible difference in how men and women perceive the subward. In Hananasif, an inner city subward near the business district, women perceive the subward to be considerably more deprived than men do. In Figure 8 we show the spatial structure in the difference between how men and women view the subwards. The subwards women view as more deprived than men are mostly concentrated in the centre of the city, and the majority of the subwards which women view as less deprived are in the outer regions of the city. We suggest two reasons for the difference in perceptions: the first is personal safety, as women may perhaps feel less safe in the city centre; the second is because the centre is the location of both the central business district and many nightlife venues, which may offer better opportunities to men.

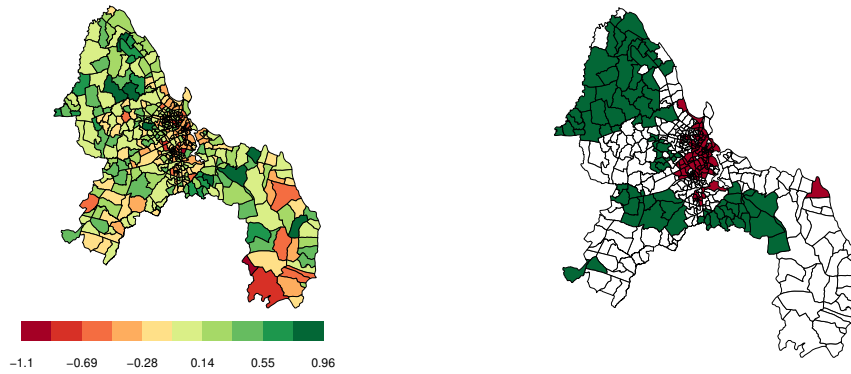


Fig. 8. The difference between men and women's views on the subwards in Dar es Salaam. Left: The posterior mean for the difference values. Green subwards are perceived to be more affluent by women compared to men, and red subwards are perceived as more deprived. Right: The difference between men and women's perceived deprivation levels, coloured by the 95% credible interval. Blank subwards have a credible interval which contains 0. Red and green subwards have a credible interval which does not contain 0, with green showing positive and red showing negative.

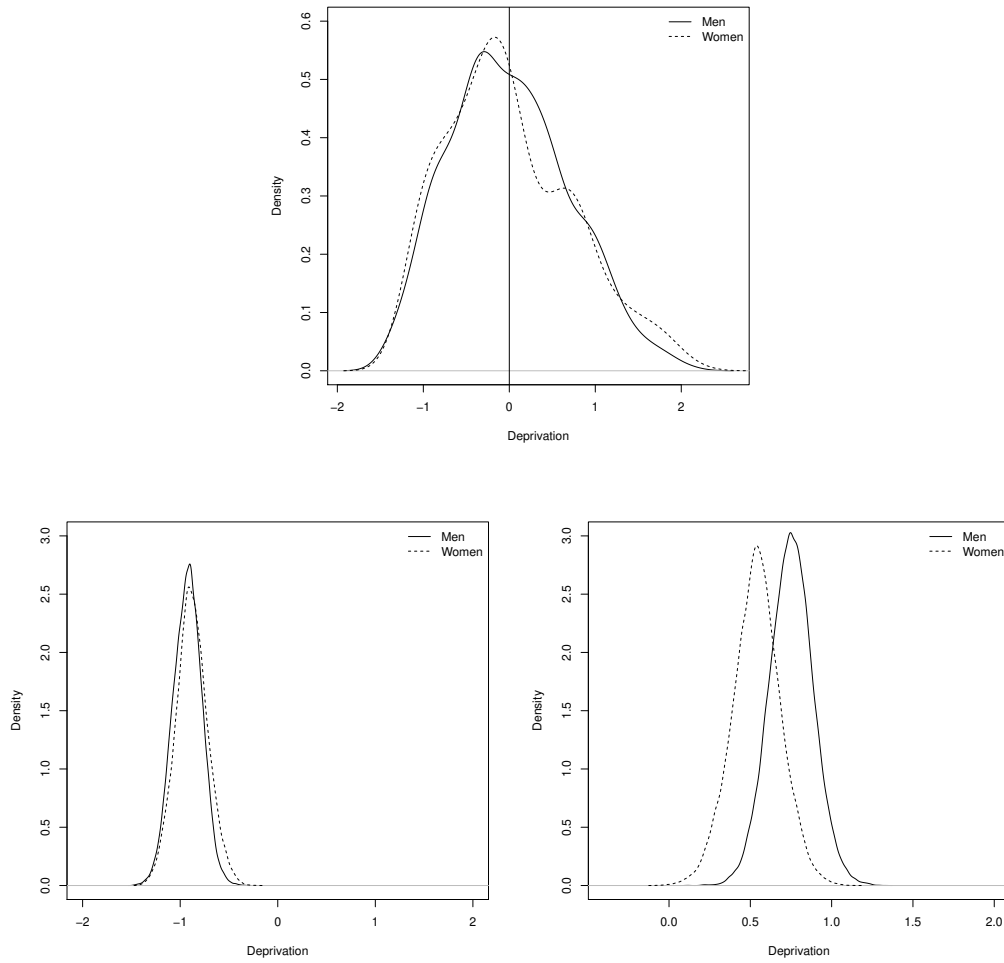


Fig. 7. Top: Kernel density estimation of posterior means for the levels of deprivation given by men and women. Bottom: The posterior distributions for the men's and women's perceptions of Kibonde Maji A (left) and Hananasif (right). We do not infer a difference between how men and women perceive Kimbanguile, but we do for Hananasif.

5. Discussion

We have developed new methods for efficiently estimating the level of deprivation in urban areas based on comparative judgement data. Existing comparative judgement models require a large amount of data to produce high quality results and collecting such quantities of data is often difficult or infeasible when working in developing countries, where data collection can be prohibitively expensive and time-consuming. Using the Bayesian Spatial Bradley–Terry model, we could have collected considerably fewer comparisons without affecting the quality of our results. When using the data collected only on the first two days on the fieldwork, the error in the BSBT model is small, and substantially smaller than when using the standard model. We achieved this by including a spatial element in the model, where the level of deprivation in one subward is correlated with the level in nearby subwards. We modelled the spatial structure using a multivariate normal prior distribution with a covariance matrix based on the network structure of the city, which avoids making rigid parametric assumptions. We also show how our method can be used to analyse how different genders perceive the level of deprivation in different areas, and how different their perceptions are. This can help researchers identify areas where one gender may be facing specific problems.

The advantages of the BSBT model are grounded in data-efficiency rather than computational gains, given the importance of the former relative to the latter in development settings (computation now being relatively cheap even in developing economies, whose digital infrastructures are often far superior to their physical ones). While the BSBT model is more computationally expensive than the standard BT model, the reduction in time and expense required for data collection far outweighs the increase in time required for computation. For the Dar es Salaam data set, the standard BT model took around 5 minutes to run whereas the BSBT model took around 4.5 hours. There is scope to reduce the computational time required by developing a more efficient MCMC algorithm, for example by adaptive updating of the underrelaxed tuning parameter δ . The BSBT model produces an estimate for the overall level of deprivation in each area; however, it is of practical interest in future to separate out the different contributing factors, for example health or educational deprivation.

We analysed a novel data set on deprivation in Dar es Salaam, not only estimating the level of deprivation in the city’s 452 subwards, but demonstrating the effectiveness of the BSBT model to significantly reduce data requirements in practice. As far as we are aware, no estimates for deprivation on such a fine scale are currently available. We were able to identify slums in the centre of the city and estimate the level of deprivation in the peri-urban outer regions of the city. Our findings show that there are several sharp changes in the level of deprivation in the centre of the city where very affluent areas neighbour slums. There is also a difference in how men and women view some areas; specifically we find that women view some parts of the centre of Dar es Salaam as more deprived than men do, but tend to view some parts of the outer regions of the city as less deprived than men do. The foregoing survey, modelling and analysis provides up-to-date estimates of deprivation levels in Dar es Salaam via the involvement of over 200 of the citizens of the city.

6. Acknowledgements

This work was supported by the Engineering and Physical Sciences Research Council [grant reference EP/T003928/1]. We also thank the Humanitarian OpenStreetMap Team (HOT) for their support in data collection.

References

- Bradley, R. A. and Terry, M. E. (1952) Rank analysis of incomplete block designs: I. the method of paired comparisons. *Biometrika*, **39**, 324–345.
- Cattelan, M. (2012) Models for paired comparison data: A review with emphasis on dependent data. *Statistical Science*, 412–433.
- Cormen, T. H., Stein, C., Rivest, R. L. and Leiserson, C. E. (2001) *Introduction to Algorithms*. Cambridge, MA: MIT Press, 2nd edn.
- Devarajan, S. (2013) Africa’s statistical tragedy. *Review of Income and Wealth*, **59**, S9–S15. URL: <https://doi.org/10.1111/roiw.12013>.
- Engelmann, G., Smith, G. and Goulding, J. (2018) The unbanked and poverty: Predicting area-level socio-economic vulnerability from m-money transactions. In *2018 IEEE International Conference on Big Data (Big Data)*, 1357–1366. IEEE.
- Estrada, E. and Higham, D. J. (2010) Network properties revealed through matrix functions. *SIAM Review*, **52**, 696–714. URL: <https://doi.org/10.1137/090761070>.
- van Etten, J., de Sousa, K., Aguilar, A., Barrios, M., Coto, A., Dell’Acqua, M., Fadda, C., Gebrehawaryat, Y., van de Gevel, J., Gupta, A., Kiros, A. Y., Madriz, B., Mathur, P., Mengistu, D. K., Mercado, L., Mohammed, J. N., Paliwal, A., Pè, M. E., Quirós, C. F., Rosas, J. C., Sharma, N., Singh, S. S., Solanki, I. S. and Steinke, J. (2019) Crop variety management for climate adaptation supported by citizen science. *Proceedings of the National Academy of Sciences*, **116**, 4194–4199. URL: <https://doi.org/10.1073/pnas.1813720116>.
- Firth, D. (2020) *qvcalc: Quasi Variances for Factor Effects in Statistical Models*. R package version 1.0.2.
- Gelman, A. (2006) Prior distributions for variance parameters in hierarchical models (comment on article by browne and draper). *Bayesian Anal.*, **1**, 515–534. URL: <https://doi.org/10.1214/06-BA117A>.
- Grinfeld, J., Nangalia, J., Baxter, E. J., Wedge, D. C., Angelopoulos, N., Cantrill, R., Godfrey, A. L., Papaemmanuil, E., Gundem, G., MacLean, C. et al. (2018) Classification and personalized prognosis in myeloproliferative neoplasms. *New England Journal of Medicine*, **379**, 1416–1430.
- Higham, N. J. (1988) Computing a nearest symmetric positive semidefinite matrix. *Linear Algebra and its Applications*, **103**, 103–118. URL: [https://doi.org/10.1016/0024-3795\(88\)90223-6](https://doi.org/10.1016/0024-3795(88)90223-6).
- Kalton, G. and Schuman, H. (1982) The effect of the question on survey responses: A review. *Journal of the Royal Statistical Society. Series A (General)*, **145**, 42–73. URL: <http://www.jstor.org/stable/2981421>.

- Kleijn, B. and van der Vaart, A. (2012) The Bernstein-von-Mises theorem under misspecification. *Electronic Journal of Statistics*, **6**, 354–381. URL: <https://doi.org/10.1214/12-ejs675>.
- Limbumba, T. M. and Ngware, N. (2016) Informal Housing Options and Locations for Poor Urban Dwellers in Dar es Salaam City. *The Journal of Social Sciences Research*, **2**, 93–99.
- Lynn, P. and Clarke, P. (2002) Separating refusal bias and non-contact bias: evidence from uk national surveys. *Journal of the Royal Statistical Society: Series D (The Statistician)*, **51**, 319–333.
- McCrickard, L. S., Massay, A. E., Narra, R., Mghamba, J., Mohamed, A. A., Kishimba, R. S., Urrio, L. J., Rusibayamila, N., Magembe, G., Bakari, M., Gibson, J. J., Eidex, R. B. and Quick, R. E. (2017) Cholera mortality during urban epidemic, Dar es Salaam, Tanzania, August 16, 2015–January 16, 2016. *Emerging Infectious Diseases*, **23**.
- McLennan, D., Noble, S., Noble, M., Plunkett, E., Wright, G. and Gutacker, N. (2019) The English indices of deprivation 2019. *Tech. rep.*, Ministry of Housing, Communities and Local Government, London, UK. URL: https://assets.publishing.service.gov.uk/government/uploads/system/uploads/attachment_data/file/833951/IoD2019_Technical_Report.pdf.
- Napacho, Z. A. and Manyele, S. V. (2010) Quality assessment of drinking water in Temeke District (part II): Characterization of chemical parameters. *The Journal of Social Sciences Research*, **4**, 775–789.
- Neal, R. M. (1998) Suppressing random walks in Markov Chain Monte Carlo using ordered overrelaxation. In *Learning in Graphical Models*, 205–228. Springer Netherlands.
- Randall, S. and Coast, E. (2015) Poverty in african households: the limits of survey and census representations. *The Journal of Development Studies*, **51**, 162–177.
- Rao, P. V. and Kupper, L. L. (1967) Ties in paired-comparison experiments: A generalization of the Bradley-Terry model. *Journal of the American Statistical Association*, **62**, 194–204.
- Rasmussen, C. E. and Williams, C. K. I. (2006) *Gaussian Processes for Machine Learning*. Cambridge, Massachusetts: MIT Press.
- Seymour, R. G. and Briant, J. (2021) *BSBT*. R package version 1.1.0.
- de Soete, G. and Winsberg, S. (1993) A Thurstonian pairwise choice model with univariate and multivariate spline transformations. *Psychometrika*, **58**, 233–256.
- Springall, A. (1973) Response surface fitting using a generalization of the Bradley-Terry paired comparison model. *Journal of the Royal Statistical Society Series C*, **22**, 59–68.
- Stern, S. E. (2011) Moderated paired comparisons: a generalized Bradley-Terry model for continuous data using a discontinuous penalized likelihood function. *Journal of the Royal Statistical Society. Series C (Applied Statistics)*, **60**, 397–415.

- Strobl, C., Wickelmaier, F. and Zeileis, A. (2011) Accounting for individual differences in Bradley-Terry models by means of recursive partitioning. *Journal of Educational and Behavioral Statistics*, **36**, 135–153.
- Turner, H. and Firth, D. (2012) Bradley-Terry models in R: The BradleyTerry2 package. *Journal of Statistical Software*, **48**. URL: <https://doi.org/10.18637/jss.v048.i09>.
- United Nations Department of Economic and Social Affairs (2019) *World urbanization prospects: the 2018 revision*. New York: United Nations.
- Varin, C., Cattelan, M. and Firth, D. (2016) Statistical modelling of citation exchange between statistics journals. *Journal of the Royal Statistical Society: Series A*, **179**, 1.

Supplementary Material

1 The standard BT model for the Dar es Salaam data set

We fit the standard BT model to the Dar es Salaam data set. To fit the model we use the `BradleyTerry2` R package. This took around 5 minutes on a standard desktop PC. A map of the inferred deprivation parameters from the standard BT model are shown in Figure 1. This is broadly very similar to the map shown in the main text (Figure 6) of the results for the BSBT model, though the smoothing effect of the prior is apparent in a few places (mainly near the most affluent and most deprived areas). We directly compare the results of the two models in Figure 2 in as well as how they compare to the values from the BSBT model. There is little difference between the results from the two models. As the uncertainty in the two models is measured in different ways, they are difficult to compare directly, however the uncertainty in the two models is of the same order and there is a clear pattern of subwards with relatively high/low uncertainty under one model also having relatively high/low uncertainty under the other model.

2 BSBT diagnostics for the Dar es Salaam data set

We fit the BSBT model to the Dar es Salaam data set and produce the results shown in Section 4.1 of the main text. Trace plots for λ_{100} and λ_{400} and α_λ^2 are shown in Figure 3. The trace plots show the deprivation parameters converge quickly, but the variance hyperparameter is slower to converge. Based on the diagnostic plots, we consider the first 500,000 iterations as a burn-in period, and compute the posterior distributions for the model parameters from the remaining 1,000,000 iterations. The trace plots show the Markov chain is mixing well.

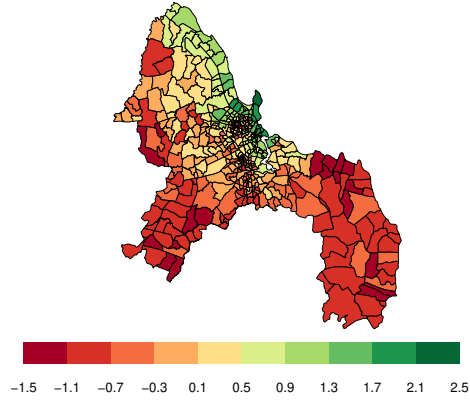


Figure 1: The results of the standard BT model applied to the full Dar es Salaam data set.

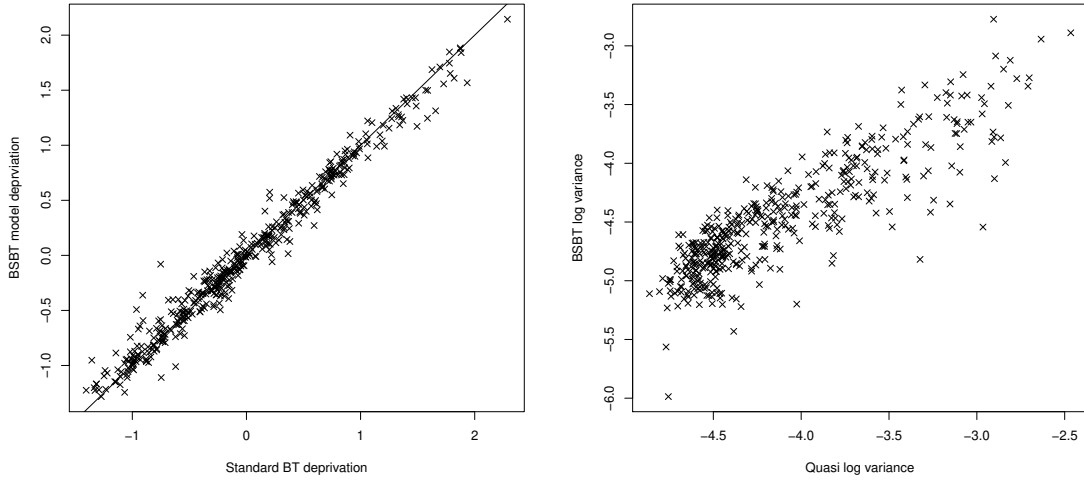


Figure 2: Left: The BSBT estimates plotted against the standard BT estimates. Right: The quasi variances for the BT model plotted against the variances of the posterior distributions for the BSBT model. Both are plotted on a log scale.

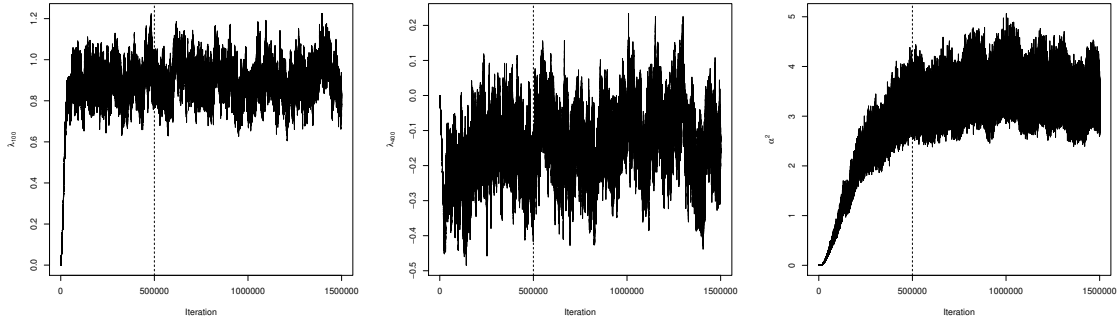


Figure 3: Trace plots for λ_{100} (left), λ_{400} (middle) and α_λ^2 (right). The dashed line is at 500,000 iterations and marks the end of the burn-in period.

3 BSBT diagnostics for the Dar es Salaam data set with gender information

We fit the BSBT model with judge information to the Dar es Salaam data set and produce the results shown in Section 4.2. Trace plots for λ_{100} , the grand mean for subward 100, $\beta_{0,100}$, the difference between men and women’s judgements in subward 100, α_λ^2 and α_1^2 are shown in Figure 4. As we ran the MCMC algorithm for 5,000,000 iterations, we thin the results to reduce the required memory and store every 50th iteration. We take the 35,000th thinned iteration to be the end of the burn-in period. The mixing could be improved, particularly for α_1^2 , which could be achieved by using adaptive MCMC and adapting the underrelaxed tuning parameter, δ .

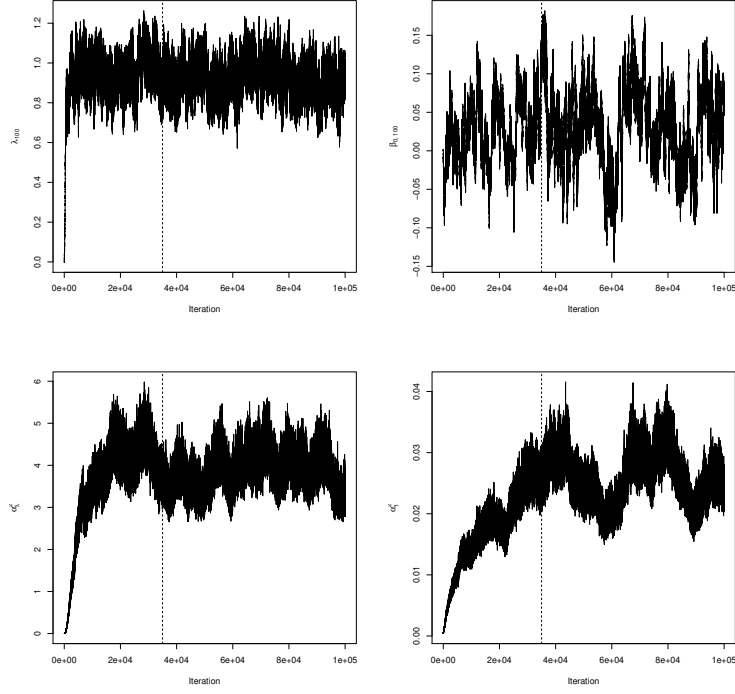


Figure 4: Trace plots for λ_{100} (top left), $\beta_{0,100}$ (top right), α_{λ}^2 (bottom left) and α_1^2 (bottom right). The 5 million iterations have been thinned to 100,000 and the dashed line at 35,000 iterations marks the end of the burn-in period.